IRSTI 31.19.15 https://doi.org/10.26577/ijbch.2020.v13.i2.14

I.Yu. Silachyov

Institute of Nuclear Physics, Almaty, Kazakhstan
e-mail: silachyov@inp.kz

Neutron activation analysis of rare earth raw material using a planar detector and thorium as an internal standard

Abstract: The application of comparator instrumental neutron activation analysis (INAA) combined with the internal standard method and counting of the induced activity by a planar type HPGe detector was considered to determine eleven lanthanides by the long-lived radionuclides in some types of rare earth and rare metal ores. The enhanced thorium contents of these objects made possible to use it as an internal standard in comparator INAA. Thorium mass fractions of the samples were determined by the method of instrumental gamma-spectrometry with the relative standard uncertainty less than 4% (P = 0.68). Four samples of geological reference materials (rocks, including a uranium-bearing rock) certified for rare earth element (REE) contents were used to verify accuracy of the method. The proposed variant of comparator INAA was shown to insure accuracy of routine analysis of the corresponding geological objects for REE contents by the III category of precision according to the industrial standard OST 41-08-221-04 (Russian Federation). To test the method twenty thorium-enriched samples from Shock-Karagai rare earth deposit (North Kazakhstan) and several similar rare metal ore samples were analyzed for lanthanide contents.

Key words: lanthanides, neutron activation analysis, internal standard.

Introduction

Instrumental neutron activation analysis (INAA) proved itself as one of the most effective methods of geological sample analysis for element contents long ago [1]. Despite the continued dynamic development of the alternative methods of elemental analysis [2] INAA is still widespread to solve a range of geochemical tasks from rock characterization [3-6] to identification of metallogenic provinces [7].

One of the most important INAA applications in geochemistry should be associated with the solution of such a difficult problem as individual lanthanide analysis [8-12]. Different investigators repeatedly emphasized undoubted advantages of INAA comparing with the other up-to-date instrumental methods of rock analysis for lanthanide contents [4, 13-15]. INAA is mostly known to get the benefit from rare earth element (REE) determination at the levels far lower their Clarke (crust average) contents, from the absence of sample decomposition and hence the need of chemical blank evaluation, clear and generally minimal matrix effect, insignificant spectral interferences and reasonable cost of the analysis. Typical rocks being analyzed by INAA, corrections for uranium fission products are usually small, and neutron flux self-shielding by major elements is practically absent.

In the case of REE analysis, main disadvantage of INAA by the long-lived radionuclides consists in its long duration, no less than 30 days after sample irradiation, to guarantee complete decay of ^{153}Sm (a spectral interference of ^{153}Gd).

All the long-lived radionuclides – the products of lanthanides activation – are characterized by rather low-energy analytical gamma-lines the most high-energy of which belongs to ^{40}La (328.8 keV). This makes possible to use in INAA a planar type semiconductor detector distinct from a coaxial one in higher detection efficiency of low-energy gamma radiation, far better energy resolution, and lower background of Compton continuum [10]. Moreover, gadolinium content being determined by radionuclide ^{161}Tb (25.7 keV), analysis can be carried out 1–2 weeks earlier.

Soon after becoming commercially available, high purity (HP) Ge planar type detectors found their broad application to analyze rocks [16, 17], chondrites [18], river sediments [19], etc. for REE contents by INAA. After getting access to the high-effective coaxial detectors with HPGe crystals of big volumes (≥200 cm^3), taking into account their higher cost, the planar type detectors were

continually used as additional ones to determine a wide range of elements including lanthanides in chondrites [20], rock reference materials [21], to study continental shelf sediments [22] and so on.

Widespread and convenient k_0-method as a variant of comparator INAA had long been recognized for concentration standardization [23]. Although it doesn't need certified reference materials (CRMs) to calibrate gamma spectrometers, k_0-method is not deprived of some drawbacks because the comparator (an Au-containing sample) is used as an external standard [13]. All the advantages of comparator INAA can be realized only by joint application of the internal standard method [24] and an independent method to analyze the element used as the comparator [25].

Iron is often selected as the internal standard to implement comparator INAA of different rock samples [26], while its content can be conveniently determined by X-ray fluorescence method (XRF) [13, 25]. A planar type detector measures ^{59}Fe count rate by the 192.3 keV gamma-line with 3.1% of the quantum yield. Insufficient intensity of this line restricts application of iron as the internal standard within its content of the samples no less than ≈5%. Other comparators being used, particularly – thorium the enhanced contents of which often accompany REE deposits [27], the range of the objects accessible for analysis could be substantially expanded.

In this work comparator INAA using a planar type detector was tried to analyze eleven lanthanides in the thorium-enriched objects such as REE and rare metal ores. Instrumental gamma-spectrometry (IGS) was used to measure thorium content of the samples since this method usually provides the higher precision of thorium determination than XRF.

Materials and methods

To implement INAA about 100 mg of the investigated rock samples ground to the particle size ≈0.07 mm were sealed in plain double polyethylene bags (approximately 1 mm of the sample thickness) and stacked up in aluminium foil. Every package prepared for a separate irradiation included ten assays and a zirconium monitor of the neutron flux (10 mg of ZrO_2) placed in the middle. Package length was about 10 mm.

All the packages were irradiated for 2.5 h in the position № 4 inside the peripheral vertical channel № 10-6 of the light-water research reactor WWR-K (Almaty, Kazakhstan) by the thermal neutron flux density 8.9×10^{13} cm^{-2} s^{-1}; the fast neutron flux density amounted to 6.0×10^{12} cm^{-2} s^{-1} [28]. The selected time of activation was based on the previous experience of typical rock sample investigations using the same facilities. To reduce the influence of the gradient of neutron spectrum composition, the packages were oriented along the channel axis. In this case the radial component of the gradient (8.5% per 1 cm) was the same for all irradiated assays and the axial one (1.2% per 1 cm) can be neglected.

Gamma-spectrometric measurements of the studied assays were conducted several times: after 6–7 days of decay (to determine La, Sm, and Ho), 12–13 days (to determine Nd, Lu, and Gd), and after 3 weeks (to determine Ce, Eu, Tb, Yb, Tm). Counting time was about 30 min, 40 min, and 1 h, correspondingly. The distance from the assay bags to the detector cap amounted to 40 mm ("far" geometry) for the first counting and 10 mm for the others two. The irradiated samples were counted by a planar HPGe detector GLP36360 with the crystal dimensions 36×13 mm and an energy resolution of 585 eV at the 122 keV peak of ^{57}Co connected to an ORTEC multi-channel analyzer DSPEC LF. MAESTRO software by ORTEC was used for the spectra collection. Detector calibration for relative detection efficiency $\varepsilon(E)$, where E is a gamma-ray energy, was made with the help of a multi-gamma ray standard MGS-1 (^{152}Eu, ^{154}Eu, ^{155}Eu) and an isotopic source ^{133}Ba, both by Canberra. $\varepsilon(E)$ values were evaluated in the interval from the weighted energy 30.85 keV of Cs$K\alpha_1$ and Cs$K\alpha_2$ X-ray lines (^{133}Ba) to 411.12 keV (^{152}Eu). A fourth power polynomial was used to fit the calibration curve.

Spectra treatment was carried out by "AnalGamma" software developed in the Institute of Nuclear Physics. The software approximates a part of gamma-ray spectrum in the treatment window by Gaussian curves and a flat background and calculates peak count rates in cps. Partly overlapping peaks can be reliably resolved. Quality of the approximation is checked by the χ^2 test.

Main nuclear parameters of the analytical gamma-lines of the radionuclides used to determine lanthanide content (including thorium as the internal standard) and the accounted interferences are presented in Table 1. If more than one line can be used for analysis preference was given to the cases of higher count rate (taking account of the detection efficiency) and minor peak overlapping. Thus, the same gamma-lines as the usually recommended

ones (e.g. [10]) were used for ^{152}Eu and ^{177}Lu counting. The part of ^{177}Lu count rate resulted from ^{176}Yb by the (n, γ) reaction was evaluated using the basic equation of activation [10]. With the Yb to Lu relation corresponding to their Clarke contents ^{176}Yb contribution to ^{177}Lu activity after 2.5 h of irradiation is ≈1.7% and can be neglected. The low-energy ^{153}Sm gamma-line was selected to avoid spectral interference by ^{233}Pa due to the thorium high contents. The same reason prevailed in the case of terbium determination by ^{160}Tb; the latter is accounted for a ^{233}Pa gamma-line only if thorium content exceeds that of terbium by more than one order of magnitude. The most intensive gamma-line of ^{169}Yb (63.12 keV) is overlapped by a ^{177}Lu gamma-line only to a small extent. U(n, f) means that an analyzed radionuclide (^{40}La and others) is produced by the fission of the uranium containing in the sample. ^{133}Xe is a uranium fission product too, but it was accounted as a spectral interference. Other interferences in the similar aluminum-siliceous matrixes are insignificant and hence were ignored.

Table 1 – Main nuclear parameters and interferences of the radionuclides used to calculate lanthanides by INAA internal standard method

Radionuclide	Half-life, days	Energy, keV	Quantum yield, %	Interferences	Energy, keV	Quantum yield, %
^{140}La	1.7	328.76	20.3	U(n,f)	-	-
^{141}Ce	32.5	145.44	48.3	U(n,f)	-	-
^{147}Nd	11.0	91.11	28.1	U(n,f)	-	-
^{153}Sm	1.9	69.67	4.73	^{187}W	69.31	3.17
^{152}Eu	4943	121.78	28.7	-	-	-
^{161}Tb (^{161}Gd)	6.9	25.65	23.2	^{122}Sb	25.27	0.95
^{160}Tb	72.3	298.58	26.1	^{233}Pa	298.81	0.088
^{166}Ho	1.1	80.57	6.71	^{133}Xe	81.00	36.9
^{170}Tm	128.6	84.25	2.48	^{182}Ta	84.68	2.65
^{169}Yb	32.0	63.12	43.6	^{177}Lu	63.24	0.599
^{177}Lu	6.6	208.37	10.4	^{176}Yb→^{177}Lu	208.37	10.4
^{233}Pa (^{233}Th)	27.0	311.90	38.5	-	-	-

Contribution coefficients F_{Ui} of uranium fission products to analyze La, Ce, and Nd contents were evaluated empirically with the help of a CRM of uranium ion solution (by Perkin Elmer). F_{Ui} values were assessed as the ratios of the count rates of the corresponding radionuclide analytical gamma-lines to the count rate of ^{239}Np (106.12 keV) under the same counting conditions.

REE ore samples were scanned at first with the help of XRF. Then the selected samples with the enhanced thorium content were analyzed by IGS. About 100 g (±0.1 g) of each assay measured by an analytical balance was placed in a cylindrical polyethylene beaker. To provide gamma-spectrometric counting a HPGe coaxial detector GX5019 (relative efficiency is 50% and an energy resolution is 1.86 keV at the 1332 keV peak of ^{60}Co) was used connected to an Canberra multi-channel analyzer. The spectrometer was calibrated for detection efficiency using a volumetric gamma-ray source – thorium ore CRM IAEA-RgTh-1 and the homemade software. Counting time of the investigated assays amounted to 3–4 h.

Thorium content was determined by the equilibrium activity of its daughter radionuclide ^{212}Pb using the 238.6 keV gamma-line, quantum yield is 43.6%, on the assumption of undisturbed secular equilibrium with the other members (^{228}Ra and ^{228}Th) of the decay chain. If the rocks were not being subjected to geochemical leaching, equilibrium in the thorium nuclear series usually maintains [29]. Moreover, due to the short half-time

of ^{220}Rn (56 s) – a predecessor of ^{212}Pb – it's no need to seal the assays.

Results and discussion

Lanthanide contents C_a (%) of the analyzed samples were calculated according to the equation of simple comparator method of standardization in INAA [30] (lower case indices *a* and *c* mean an analyzed element and the comparator, respectively):

$$C_a = C_c \frac{k_{0,c} N_{p,a} \varepsilon(E_c)(f + Q_0^c)(SD)_c}{k_{0,a} N_{p,c} \varepsilon(E_a)(f + Q_0^a)(SD)_a} K_{a,c}, \quad (1)$$

where C_c is the element comparator content of the sample (%), k_0 is k_0-factor relatively to the 411.8 keV gamma-line of radionuclide ^{198}Au for the gamma-lines of the comparator and an analyzed element [31], N_p is the net peak area of the analytical gamma-line of the corresponding radionuclide (cps), Q_0 is the resonance integral I_0 (cm^2) to the thermal neutron cross-section σ_0 (cm^2) ratio, f is the thermal to epithermal neutron flux ratio, $S = 1 - \exp(-\lambda t_{irr})$ is saturation factor depending on the irradiation time t_{irr} and decay constant λ, $D = \exp(-\lambda t_d)$ is decay factor depending on the decay time t_d after the end of irradiation. Since there is no a k_0-factor for radionuclide ^{161}Tb in the data base [31], a *k*-factor was used instead composed of the nuclear constant product:

$$k = \sigma_0 \theta P_\gamma M^{-1}, \quad (2)$$

where θ is isotopic abundance (%), P_γ is the yield of the measured gamma-line (%), M is the atomic mass (Da). Here σ_0, θ, and M relate to the activated short-lived radionuclide ^{160}Gd, and P_γ – to the gamma-line of the daughter long-lived ^{161}Tb (25.7 keV).

When INAA of rock samples for the long-lived radionuclides is carried out correction for the measuring time is always <1% and can be neglected. Neutron self-shielding of the thermal and resonance neutron flux by a 100 mg rock sample was assessed following C.Chilian, et al. [32] using a spreadsheet kindly presented by the authors. The correction factor does not exceed 1% up-to the twenty-fold excess of Gd, Sm, and Eu contents over their Clarke values. Gamma-ray self-absorption by the rock samples was evaluated using a model sample corresponding to the crust averages of the main rock-forming elements in the approximation of a thin irradiating layer [33]. Gadolinium content being analyzed by ^{161}Tb (E = 25.7 keV, Table 1) photoelectric absorption and scattering [34] of the analytical gamma-line in a typical plane sample (1 mm of the thickness) comes up to approximately 9%. However self-absorption by the sample of the next low-energy gamma-line – ^{169}Yb (E = 63.1 keV) is lower 1%, i.e. it can be neglected.

The empirical correction factor $K_{a,c}$ is applied to compensate for an analytical bias caused by the errors of detector calibration for detection efficiency, absence of Q_0 correction for the deviation of thermal neutron flux from 1/E law, and by other reasons. In particular, using the same counting geometries, there is no need to correct J for true coincidences. $K_{a,c}$ values were assessed by the repeated irradiation and counting of the CRMs certified for REE and thorium contents.

The model resonance to thermal neutron flux ratio 1/f was evaluated using the "bare bi-isotopic method" [35] with the help of a monitor of the neutron flux spectral composition – a ZrO_2 sample [13]:

$$\frac{1}{f} = \frac{\sigma_{0,2} - B\sigma_{0,1}}{BI_{0,1} - I_{0,2}}, \qquad B = \frac{N_{p,2} \varepsilon(E_1) \theta_1 P_{\gamma,1} (SD)_1}{N_{p,1} \varepsilon(E_2) \theta_2 P_{\gamma,2} (SD)_2}, \quad (3)$$

where lower indices 1 and 2 correspond to two Zr isotopes ($Q_{0,1} << Q_{0,2}$). During the investigation 1/f values in the irradiation position varied within the small range 0.029–0.034.

To assess accuracy of lanthanide determination by comparator INAA the following four rock CRMs certified for REE content were selected thorium content of which was sufficient to apply IGS: SG-4 (Russian Federation), GBW-07110 (China), DC-73301 (China), and OREAS 100a (Australia). REE mass fractions of these CRMs ranged from approximately Clarke ones (DC-73301) to several Clarke values (OREAS 100a) (Tables 2–5). The CRM samples were prepared, irradiated and analyzed as described above. To avoid overirradiation the assay mass of OREAS 100a was diminished to 50 mg. A single measurement of each CRM was carried out.

Uranium content of DC-73301 reaches 18.8 μg/g and comes up to 135 μg/g in OREAS 100a. GBW-07110 is characterized by a negligible

contribution of uranium fission products to the count rate of La analytical gamma-line and a minimum contribution to Ce and Nd gamma-lines, no more than 1–1.5%. In case of OREAS 100a analysis the corresponding correction reached 10% for Ce, 16% for Nd and 1% for La.

As for the other spectral interferences presented in Table 1, W contribution to Sm analytical gamma-line count rate ranged within 1.5–2.5%, Ta to Tm – from 29% (SG-4) to 68% (DC-73301), and Lu to Yb – within 2.5–6%. ^{133}Xe contribution to the area of unresolved double peak ^{166}Ho + ^{133}Xe came up to 24–25% for GBW-07110 and SG-4, and 48% for DC-73301 after 7 days of the decay time. The corresponding contribution reached 59.5% in case of OREAS 100a counting 6 days after irradiation. Due to Sb low content, 2.5 μg/g of OREAS 100a and no more than 1.3 μg/g of the other CRMs, contribution of Sn$K\alpha_1$ X-ray line resulting from ^{122}Sb decay (Table 1) to ^{161}Tb gamma-line was neglected.

Expanded uncertainty of the INAA results was estimated as follows (P = 0.95):

$$U(C_a) \approx \approx 2C_a\sqrt{\frac{u(J_a)^2}{J_a^{\,2}}+\frac{u(J_c)^2}{J_c^{\,2}}+\frac{u(C_c)^2}{C_c^{\,2}}+\delta_a^{\,2}}, \quad (4)$$

where $u(J_a)$, $u(J_c)$, and $u(C_c)$ are standard uncertainties of the corresponding values as in Eq. 1, δ_a is the standard deviation of element analysis (methodical uncertainty) by comparator INAA (all the ratios and δ_a are in %). δ_a values were assessed earlier with the help of the CRMs and ranged from 2.6% (Eu determination) to 5.0% (determination of Ho and Tm). Relative standard uncertainty of the ^{233}Pa analytical gamma-line count rate amounted to <2%.

To assess relative standard uncertainty (%) of thorium content determination by IGS the next expression was used (P = 0.68):

$$\frac{u(C_c)}{C_c} \approx \approx \sqrt{\frac{u(J_a)^2}{J_a^{\,2}}+\frac{u(J_r)^2}{J_r^{\,2}}+\frac{u(C_r)^2}{C_r^{\,2}}+\delta_m^{\,2}}, \quad (5)$$

where $u(J_a)$ and $u(J_r)$ are standard (statistical) uncertainties of the ^{212}Pb analytical gamma-line count rates of the investigated sample and CRM IAEA-RgTh-1 (P = 0.68), $u(C_r)$ is standard uncertainty of the thorium certified content C_r of IAEA-RgTh-1(1%, P = 0.68), δ_m is relative methodical uncertainty resulting from measuring of the cylindrical assay height (≈1%). Relative standard uncertainty of ^{212}Pb analytical gamma-line count rate never exceeded 2.5%. So, relative standard uncertainty of thorium comparator determination was no more than 4% (P = 0.68).

The results of four CRM analyses for lanthanide contents by comparator INAA including thorium content by IGS are presented in Tables 2–5.

Table 2 – REE contents of SG-4 (subalkaline granite) by comparator INAA, μg/g (P = 0.95)

Element	Certified value	Measured value	E_n-number
La	91 ± 7	86.0 ± 8.2	-0.47
Ce	177 ± 27	191 ± 17	0.44
Nd	84 ± 14	84.6 ± 8.5	0.04
Sm	19 ± 3	17.3 ± 1.7	-0.49
Eu	0.64 ± 0.06	0.64 ± 0.05	0.01
Gd	15 ± 2	15.1 ± 1.7	0.04
Tb	2.5 ± 0.3	2.59 ± 0.26	0.23
Ho	2.6 ± 0.5	2.48 ± 0.35	-0.20
Tm	1.1 ± 0.2	1.18 ± 0.15	0.32
Yb	7.4 ± 1.4	7.95 ± 0.82	0.34
Lu	1.3 ± 0.3	1.31 ± 0.13	0.03
Th	20 ± 3	20.1 ± 1.4	0.04

Table 4 – REE contents of DC-73301 (rock) by comparator INAA, μg/g (P = 0.95)

Element	Certified value	Measured value	E_n-number
La	54 ± 4	53.7 ± 4.8	-0.05
Ce	108 ± 7	106 ± 10	-0.17
Nd	47 ± 4	44.0 ± 4.4	-0.50
Sm	9.7 ± 0.8	9.57 ± 0.91	-0.11
Eu	0.85 ± 0.07	0.83 ± 0.07	-0.19
Gd	9.3 ± 0.7	9.1 ± 1.2	-0.18
Tb	1.65 ± 0.09	1.67 ± 0.17	0.10
Ho	2.05 ± 0.17	2.08 ± 0.29	0.09
Tm	1.06 ± 0.09	0.99 ± 0.12	-0.49
Yb	7.4 ± 0.5	7.32 ± 0.75	-0.09
Lu	1.15 ± 0.09	1.11 ± 0.12	-0.27
Th	54 ± 3	53.9 ± 3.5	-0.02

Table 3 – REE contents of GBW-07110 (trachyte andesite) by comparator INAA, μg/g (P = 0.95)

Element	Certified Value	Measured value	E_n-number
La	62.5 ± 2.5	61.9 ± 5.8	-0.09
Ce	117 ± 7	121 ± 11	0.31
Nd	47.2 ± 2.5	49.0 ± 4.9	0.33
Sm	8.63 ± 0.23	8.60 ± 0.86	-0.03
Eu	1.96 ± 0.07	2.03 ± 0.16	0.40
Gd	6.54 ± 0.40	6.37 ± 0.92	-0.17
Tb	0.99 ± 0.07	0.99 ± 0.11	0.04
Ho	1.1 ± 0.1	1.12 ± 0.19	0.10
Tm	0.50 ± 0.04	0.463 ± 0.073	-0.44
Yb	3.15 ± 0.10	3.12 ± 0.32	-0.09
Lu	0.49 ± 0.04	0.511 ± 0.052	0.32
Th	16.7 ± 0.6	16.2 ± 1.1	-0.41

The measured thorium internal standard contents are well comparable with the certified ones within ≤3% of discrepancy. All the lanthanides analyzed mass fractions differ from their certified contents by no more than 10%. Expanded uncertainty of lanthanides analysis in all the four CRMs $U(C_a)$ by comparator INAA doesn't exceed the allowable standard deviation of the results of their determination directed by the III category of precision (of analysis) according to OST 41-08-221-04 [36].

E_n-number of lanthanides determination was additionally evaluated as a criterion recommended by IUPAC to verify the laboratory performance [37]:

$$E_n = \frac{C_a - C_r}{\sqrt{U(C_a)^2 + U(C_r)^2}}, \qquad (6)$$

where $U(C_r)$ is expanded uncertainty of the analyzed element certified value C_r (P = 0.95). E_n-number values within $-1<E_n<1$ interval are considered admissible if the relative deviation $C_a - C_r$ doesn't exceed a predetermined quantity. In the present investigation maximum deviation ±10% was accepted.

Table 5 – REE contents of OREAS 100a (uranium-bearing rock) by comparator INAA, μg/g (P = 0.95)

Element	Certified Value	Measured value	E_n-number
La	260 ± 8	269 ± 25	0.34
Ce	463 ± 20	477 ± 43	0.30
Nd	152 ± 8	156 ± 15	0.24
Sm	23.6 ± 0.4	24.2 ± 2.4	0.25
Eu	3.71 ± 0.23	3.89 ± 0.31	0.47
Gd	23.6 ± 1.4	23.5 ± 2.9	-0.03
Tb	3.80 ± 0.23	3.82 ± 0.38	0.05
Ho	4.81 ± 0.14	4.99 ± 0.66	0.27
Tm	2.31 ± 0.12	2.22 ± 0.27	-0.30
Yb	14.9 ± 0.4	14.9 ± 1.5	0.00
Lu	2.26 ± 0.11	2.37 ± 0.26	0.39
Th	51.6 ± 2.7	52.4 ± 3.3	0.19

Since E_n-number absolute values appeared less than unity (Tables 2–5) and the relative bias – less than 10%, the results of lanthanide analysis can be considered acceptable by E_n-number criterion too.

So the opportunity to use comparator INAA by long-lived radionuclides with a planar type HP Ge detector and thorium as the internal standard to analyze the rock CRMs for lanthanide contents was demonstrated. Then to verify this approach it was tried for real geological objects.

One of them is the rare earth deposit Shock-Karagai in North Kazakhstan, a part of the big complex rare metal and rare earth province Syrymbet. Industrially significant agglomerations of REEs in the deposit are associated with the weathering crusts and Cenozoic loose sediments. Placers are enriched with the light lanthanides and accompanied by thorium increased contents 0.008–0.02% [38].

The results of eleven lanthanides determinations in twenty REE ore samples by comparator INAA (P = 0.95) are presented in Table 6. Preliminary elemental analysis of the core material was carried out by XRF. All the samples are characterized by relatively low iron mass fractions 0.5–3.3%, insufficient to measure ^{59}Fe count rate by a planar detector in the "far" geometry with the necessary statistical uncertainty. Thorium content of the samples is high enough and therefore was determined by IGS.

The ratio of sum contents of the cerium and yttrium groups (Table 6) confirms the conclusion that the light lanthanides are characteristic of the Shock-Karagai weathering crust [38] unlike that of some other Kazakhstan's REE deposits. Several samples such as 2001/5, 7005/14, 7008/12 and TT-2 are distinguished by the enhanced relative sum mass fraction of the heavy REEs.

It may be noted that a high enough value of the thermal neutron cross-section and monoisotopic composition makes possible to use thorium as an internal standard in comparator INAA beginning from its Clarke contents. This opportunity is restricted only by the sensitivity of thorium determination by an independent method. Neutron activation analysis of the REE ores characterized by thorium enhanced mass fractions for lanthanide contents causes no difficulties and may be regarded as a major application of the planar type detectors in comparator INAA.

Typical gamma-ray spectra of an REE ore sample (№ 7004/2) are presented in Fig. 1 in a log-linear scale after 7 days (a) and 3 weeks (b) of decay. The first spectrum was counted for 35 min and the second one – for about 50 min. Fig. 1(b) displays a low-energy part of the spectrum with the analytical lines of ^{169}Yb and ^{170}Tm. GLP36360 doesn't discriminate between ^{170}Tm and ^{182}Ta gamma-peak energies (84.3 and 84.7 keV) but it resolves the sum peak up to the background, unlike coaxial detectors. Gamma-lines of ^{160}Tb (298.6 keV) and ^{233}Pa (300.1 keV) partly resolved by the planar detector are usually reliably divided by the software even when thorium content of the samples exceeds 100 μg/g. Despite the much lower count rate of 298.6 keV gamma-line comparing with 86.8 keV one of ^{160}Tb, the latter was not chosen as the analytical line because of the frequently fallible results caused by ^{233}Pa spectral interference (86.6 keV). ^{152}Eu and ^{141}Ce gamma-lines are not shown in Fig. 1(b) since there is no problem with corresponding element determination.

Table 6 – Lanthanides and thorium contents of the Shock-Karagai REE ore samples by comparator INAA, μg/g ($P = 0.95$)

Sample	Th	La	Ce	Nd	Sm	Eu	Gd	Tb	Ho	Tm	Yb	Lu
463	41.3 ± 2.1	103 ± 10	209 ± 21	98.7 ± 9.9	21.2 ± 2.1	1.31 ± 0.13	17.5 ± 1.4	3.06 ± 0.31	3.91 ± 0.45	1.53 ± 0.18	10.6 ± 1.1	1.60 ± 0.16
2001/5	41.8 ± 2.1	88.5 ± 8.9	146 ± 15	60.6 ± 6.6	12.2 ± 1.2	0.56 ± 0.06	12.4 ± 1.2	2.75 ± 0.28	3.38 ± 0.39	1.69 ± 0.19	12.3 ± 1.2	1.92 ± 0.19
7002/7	102.5 ± 5.1	171 ± 17	321 ± 32	109 ± 11	19.1 ± 1.9	0.86 ± 0.09	14.9 ± 1.5	2.53 ± 0.25	2.59 ± 0.32	0.93 ± 0.12	7.03 ± 0.70	1.04 ± 0.11
7002/8	123.9 ± 6.2	274 ± 27	494 ± 50	176 ± 18	32.2 ± 3.2	1.38 ± 0.14	26.9 ± 2.7	4.58 ± 0.46	4.68 ± 0.55	1.48 ± 0.18	9.64 ± 0.95	1.38 ± 0.14
7002/9	107.1 ± 5.4	225 ± 23	403 ± 40	144 ± 15	26.1 ± 2.6	1.17 ± 0.12	23.8 ± 2.4	3.96 ± 0.40	3.73 ± 0.44	1.38 ± 0.16	8.71 ± 0.87	1.24 ± 0.13
7002/12	45.2 ± 2.4	76.5 ± 6.9	113 ± 10	58.3 ± 5.8	11.8 ± 1.2	0.55 ± 0.05	11.4 ± 1.3	2.28 ± 0.23	3.21 ± 0.40	1.56 ± 0.20	10.8 ± 1.1	1.69 ± 0.17
7004/2	70.5 ± 3.5	113 ± 11	314 ± 32	86.3 ± 8.6	15.8 ± 1.6	2.06 ± 0.21	13.6 ± 1.4	2.22 ± 0.22	2.48 ± 0.29	0.81 ± 0.11	6.86 ± 0.69	1.09 ± 0.11
7004/5	82.7 ± 4.1	96.1 ± 9.6	198 ± 20	58.2 ± 5.8	11.8 ± 1.2	0.55 ± 0.06	11.4 ± 1.1	2.09 ± 0.21	2.52 ± 0.29	0.69 ± 0.10	5.63 ± 0.56	0.83 ± 0.08
7004/10	65.4 ± 3.3	915 ± 92	601 ± 60	473 ± 47	88.5 ± 8.9	3.86 ± 0.39	83.6 ± 8.4	13.8 ± 1.4	12.2 ± 1.4	3.64 ± 0.41	20.4 ± 2.1	2.84 ± 0.29
7005/6	103.1 ± 5.2	68.8 ± 6.9	236 ± 24	47.5 ± 4.8	8.60 ± 0.86	0.45 ± 0.05	8.23 ± 0.98	1.51 ± 0.15	1.85 ± 0.23	0.69 ± 0.12	6.78 ± 0.68	1.07 ± 0.11
7005/9	89.8 ± 4.5	178 ± 18	304 ± 31	126 ± 13	23.6 ± 2.4	1.20 ± 0.12	20.2 ± 2.0	3.86 ± 0.39	4.56 ± 0.52	1.94 ± 0.23	12.9 ± 1.3	1.95 ± 0.20
7005/14	63.9 ± 3.2	399 ± 40	251 ± 25	237 ± 24	45.7 ± 4.6	2.68 ± 0.27	43.2 ± 4.3	8.77 ± 0.88	12.1 ± 1.4	5.45 ± 0.60	33.8 ± 3.4	5.15 ± 0.52
7006/4	80.0 ± 4.0	674 ± 67	1080 ± 110	349 ± 35	58.5 ± 5.9	2.90 ± 0.29	46.0 ± 4.6	6.81 ± 0.68	6.14 ± 0.75	1.72 ± 0.22	10.0 ± 1.0	1.43 ± 0.15
7006/6	63.0 ± 3.2	263 ± 26	468 ± 47	158 ± 16	27.7 ± 2.8	1.23 ± 0.14	24.7 ± 2.5	4.21 ± 0.42	4.84 ± 0.57	1.67 ± 0.20	10.4 ± 1.1	1.59 ± 0.16
7006/7A	54.3 ± 2.9	169 ± 17	277 ± 28	95.7 ± 9.6	16.4 ± 1.6	0.93 ± 0.09	14.6 ± 1.5	2.69 ± 0.27	3.08 ± 0.37	1.14 ± 0.14	7.50 ± 0.75	1.14 ± 0.11
7006/8A	65.0 ± 3.3	227 ± 23	361 ± 36	130 ± 13	23.4 ± 2.4	1.14 ± 0.12	22.8 ± 2.3	3.72 ± 0.37	4.02 ± 0.47	1.49 ± 0.18	8.95 ± 0.90	1.36 ± 0.14
7007/10	64.0 ± 3.2	173 ± 17	357 ± 36	113 ± 11	20.5 ± 2.1	1.19 ± 0.13	17.2 ± 1.6	2.87 ± 0.29	2.93 ± 0.35	1.13 ± 0.16	8.18 ± 0.82	1.26 ± 0.13
7007/11	71.9 ± 3.6	778 ± 78	608 ± 61	532 ± 53	98.6 ± 9.9	6.03 ± 0.60	73.4 ± 7.5	12.4 ± 1.3	13.1 ± 1.5	4.73 ± 0.54	29.2 ± 2.9	4.24 ± 0.43
7008/12	79.8 ± 4.0	101 ± 10	116 ± 12	72.2 ± 7.2	14.4 ± 1.5	1.00 ± 0.010	13.7 ± 1.4	3.57 ± 0.36	5.88 ± 0.65	3.21 ± 0.38	24.4 ± 2.5	3.90 ± 0.39
TT-2	59.1 ± 3.0	130 ± 13	222 ± 22	70.6 ± 7.1	15.9 ± 1.6	0.34 ± 0.04	14.2 ± 1.4	3.27 ± 0.33	5.02 ± 0.55	2.37 ± 0.26	17.2 ± 1.7	2.72 ± 0.27

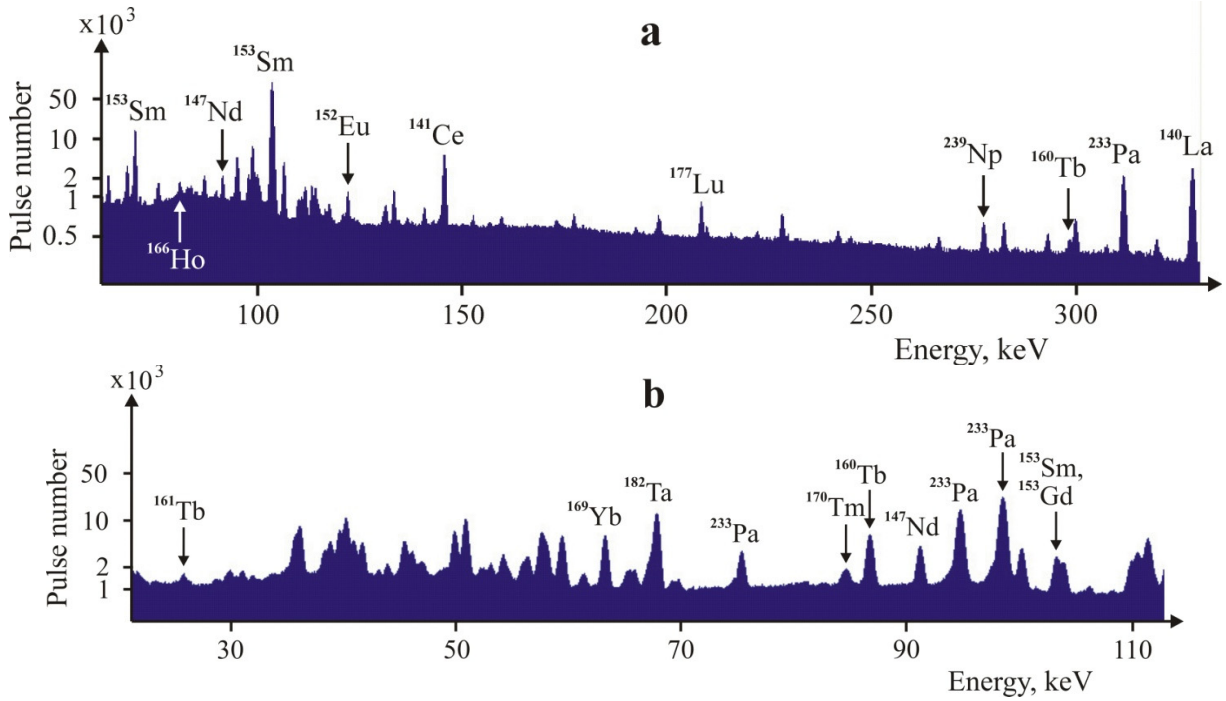

Figure 1 – Parts of the gamma-ray spectra of REE ore sample № 7004/2 counted by GLP36360 after 7 days (a) and 3 weeks (b) of decay (in a log-linear scale)

Another example of the approach verification relates to a nontraditional REE source such as rare metal deposits. As throughout the world, rare earth elements in Kazakhstan are often found in close association with zirconium, niobium, tantalum, and thorium [39]. In the absence of the samples collected from the corresponding fields, several different types of rare metal CRMs with sufficiently high thorium contents were selected for investigation. They are: GSO-2273 (a zirconium ore), NFS-15 (a tantalum-niobium-zirconium ore), both by Russian Federation, GSO-1711 (a tungsten ore, Kazakhstan), and IAEA-RgTh-1. All these CRMs were not certified for lanthanide mass fractions. Thorium content of GSO-2273 and GSO-1711 was determined by IGS and certified in the other samples. Based on preliminary analysis, to conduct INAA IAEA-RgTh-1 assay was significantly diminished to 20 mg, and the other CRM assays – to 40–50 mg.

The results of REE determination in the four rare metal ore samples by comparator INAA (P = 0.95) are presented in Table 7. Certified contents of the elements or their oxides accounting for the ore types are tabulated too. The table is supplemented with the certified or measured mass fractions of uranium since it often accompanies rare metal ores in higher contents.

In case of zirconium ore analysis, contribution of the uranium fission products to the count rate of La analytical gamma-line were negligible and reached approximately 6% and 11% to Ce and Nd ones. Sm gamma-line count rate was corrected for ≈8%. Due to a rather high tantalum content, correction to Tm gamma-line intensity amounted to 82%. ^{161}Tb count rate was increased by 8% comparing with INAA of a typical (model) rock according to the estimated self-absorption of the 25.7 keV gamma-line by zirconium.

The tungsten ore sample was analyzed in the standard manner with the exception that Sm content was found by the 103.2 keV gamma-line because of the extremely high correction of the 69.7 keV line count rate. Uranium contribution as a spectral interference to 103.2 keV gamma-line amounted to 10%.

The sample of complex tantalum-niobium-zirconium ore presented a rather difficult challenge resulted from the high contents of three interfering elements – uranium, thorium and tantalum. The former one caused substantial corrections to the intensities of La, Ce, and Nd analytical gamma-lines amounted to approximately 10%, 39% and 62%, correspondingly. Thorium contribution to Tb gamma-line count rate reached 15%. Very high correction in the case of Tm analysis (≈97%) made the result a rather approximate one.

Table 7 – Lanthanides, thorium and some basic element contents of the rare metal ore samples by comparator INAA, μg/g (P = 0.95)

Element	Zirconium ore	Tungsten ore	Tantalum-niobium-zirconium ore	Thorium ore
La	56.1 ± 5.8	16.3 ± 1.6	19.9 ± 2.0	1530 ± 140
Ce	119 ± 11	51.2 ± 5.1	63.3 ± 6.3	3640 ± 330
Nd	48.4 ± 5.1	25.6 ± 2.6	24.4 ± 3.2	1740 ± 160
Sm	8.33 ± 0.89	9.16 ± 0.85	10.6 ± 1.0	280 ± 27
Eu	1.04 ± 0.10	0.122 ± 0.011	0.119 ± 0.013	69.1 ± 5.8
Gd	7.7 ± 1.6	8.5 ± 1.0	9.2 ± 1.8	154 ± 17
Tb	1.77 ± 0.18	2.01 ± 0.20	3.97 ± 0.40	15.5 ± 1.5
Ho	3.77 ± 0.53	3.03 ± 0.32	7.6 ± 1.0	5.2 ± 1.5
Tm	1.52 ± 0.24	1.86 ± 0.23	1.0 ± 0.3	< 0.2
Yb	33.9 ± 3.4	15.8 ± 1.6	53.5 ± 5.3	2.58 ± 0.29
Lu	5.03 ± 0.48	2.76 ± 0.26	8.61 ± 0.87	0.32 ± 0.04
Zr, %	3.87 ± 0.09 [a]	-	0.35 ± 0.02 [a]	-
Nb_2O_5, %	-	-	0.199 ± 0.009 [a]	-
Ta_2O_5, %	0.0039 ± 0.0004	0.0020 ± 0.0002	0.019 ± 0.002 [a]	-
W	17.7 ± 1.8	286 ± 16 [a]	-	-
U	21.3 ± 1.9	10.0 ± 1.0	134 ± 7 [a]	6.3 ± 0.4 [a]
Th	34.6 ± 1.4	38.9 ± 1.8	740 ± 38 [a]	800 ± 16 [a]

[a] Certified value

All the three samples are characterized by the Clarke, or sub-Clarke contents of the light lanthanides and by the several times increased contents of the heavy ones, from Ho to Lu, comparing with their Clarkes. This allows considering the corresponding ore types as a valuable source of heavy lanthanide by-product production.

The thorium ore sample differs from the three above in high industrial contents of the light REEs, while the heavier ones correspond to their crust averages.

In several cases the planar detector enabled to determine the elements inaccessible to coaxial ones due to the very high thorium content. The first of them is Gd since the 103.2 keV analytical gamma-line of ^{153}Gd can't be reliably separated from the far more intensive 103.9 keV line of ^{233}Pa. The other examples include Eu and Nd determination in the sample of tantalum-niobium-zirconium ore, Yb and Lu in the thorium ore sample. These failures of the coaxial detectors result from the very poor peak-to-background ratios of the corresponding radionuclides due to their low count rates and a high Compton continuum of the spectra.

Conclusion

A variant of comparator INAA using a planar type HPGe detector and thorium as the internal standard was shown as a reliable method for eleven lanthanides analyses by the long-lived radionuclides in the REE ore samples characterized by the enhanced thorium contents and low contents of iron insufficient to use it as the internal comparator. Thorium mass fraction of the samples was conveniently found by the method of IGS insuring in this case better precision than usually used XRF. A planar type detector makes possible to determine gadolinium by the generally interference-free analytical gamma-line of ^{161}Tb (25.7 keV) thus reducing the whole time of the analyses by one-two

weeks and making free coaxial detectors for other applications.

By the example of INAA of several rock CRMs and the ore samples from the Shock-Karagai REE deposit the possibility of routine analysis of the similar objects by the III category of precision according to OST 41-08-221-04 was demonstrated.

The proposed variant of comparator INAA also suggests an advantage in the analysis of REE and thorium-containing rare metal ores comparing with the traditional application of the coaxial detectors.

Acknowledgments

The work was supported by a grant from Ministry of Education and Sciences of the Republic of Kazakhstan (BR05236400).

References

1 Hoffman E.L. (1992) Instrumental neutron activation in geoanalysis. *J Geochem Explor*, vol. 44(1-3), pp. 297-319. https://doi.org/10.1016/0375-6742(92)90053-B.

2 Bulska E., Ruszczyńska A. (2017) Analytical techniques for trace element determination. *Phys Sci Rev*, vol. 2(5). https://www.degruyter.com/view/journals/psr/2/5/article-20178002.xml (10.11.2020). https://doi.org/10.1515/psr-2017-8002.

3 Baccolo G., Clemenza M., Delmonte B., et al. (2015) Assessing the geochemical fingerprint of the 2010 Eyjafjallajokull tephra through instrumental neutron activation analysis: A trace element approach. *J Radioanal Nucl Chem*, vol. 306(2), pp. 429-435. https://doi.org/10.1007/s10967-015-4092-7.

4 Alnour I.A., Wagiran H., Ibrahim N., et al. (2015) Rare earth elements determination and distribution patterns in granite rock samples by using INAA absolute method. *J Radioanal Nucl Chem*, vol. 303(3), pp. 1999-2009. https://doi.org/10.1007/s10967-014-3756-z.

5 El-Taher A., Abdelhalim M.A.K. (2014) Elemental analysis of limestone by instrumental neutron activation analysis. *J Radioanal Nucl Chem*, vol. 299(5), pp. 1949-1953. https://doi.org/10.1007/s10967-014-2925-4.

6 Mizera J., Řanda Z., Košťák M. (2010) Neutron activation analysis in geochemical characterization of Jurassic–Cretaceous sedimentary rocks from the Nordvik Peninsula. *J Radioanal Nucl Chem*, vol. 284(1), pp. 211-219. https://doi.org/10.1007/s10967-010-0472-1.

7 Avino P., Manigrasso M., Capannesi G., et al. (2015) Classification of an area as metallogenic province: environmental importance and problems. *J Radioanal Nucl Chem*, vol. 303(3), pp. 1967-1982. https://doi.org/10.1007/s10967-014-3712-y.

8 Balaram V. (2019) Rare earth elements: A review of applications, occurrence, exploration, analysis, recycling, and environmental impact. *Geoscience Frontiers*, vol. 10, pp. 1285-1303. https://doi.org/10.1016/j.gsf.2018.12.005.

9 Akam C., Simandl G.J., Lett R., et al. (2019) Comparison of methods for the geochemical determination of rare earth elements: Rock Canyon Creek REE–F–Ba deposit case study, SE British Columbia, Canada. *GEEA*, vol. 19, pp. 414-430. https://doi.org/10.1144/geochem2018-044.

10 Stosch H.-G. (2016) Neutron activation analysis of the rare earth elements (REE) – with emphasis on geological materials. *Phys Sci Rev*, vol. 1(8). https://www.degruyter.com/view/journals/psr/2016/8/article-201662.xml (10.11.2020). https://doi.org/10.1515/psr-2016-0062.

11 Damascena K., Amaral R., dos Santos Júnior J., et al. (2015) Rare-earth elements in uranium deposits in the municipality of Pedra, Pernambuco, Brazil. *J Radioanal Nucl Chem*, vol. 304(3), pp. 1053-1058. https://doi.org/10.1007/s10967-015-3934-7.

12 Capannesi G., Rosada A., Manigrasso M., et al. (2012) Rare earth elements, thorium and uranium in ores of the North-Latium (Italy). *J Radioanal Nucl Chem*, vol. 291(1), pp. 163-168. https://doi.org/10.1007/s10967-011-1197-5.

13 Silachyov I. (2016) Rare earths analysis of rock samples by instrumental neutron activation analysis, internal standard method. *J Radioanal Nucl Chem*, vol. 310(2), pp. 573-582. https://doi.org/10.1007/s10967-016-4903-5.

14 Krishnan K., Saion E., Mohamed Kamari H., et al. (2014) Rare earth element (REE) in surface mangrove sediment by instrumental neutron activation analysis. *J Radioanal Nucl Chem*, vol. 301(3), pp. 667-676. https://doi.org/10.1007/s10967-014-3221-z.

15 Ravisankar R., Manikandan E., Dheenathayalu M., et al. (2006) Determination and distribution of rare earth elements in beach rock samples using instrumental neutron activation analysis (INAA). *Nucl Instrum Methods Phys Res B*,

vol. 251(2), pp. 496-500. https://doi.org/10.1016/j.nimb.2006.07.021.

16 Chappell B.W., Hergt J.M. (1989) The use of known Fe content as a flux monitor in neutron activation analysis. *Chem Geol*, vol. 78, pp. 151-158. https://doi.org/10.1016/0009-2541(89)90113-7.

17 Potts P.J., Thorpe O.W., Isaacs M.C., et al. (1985) High-precision instrumental neutron-activation analysis of geological samples employing simultaneous counting with both planar and coaxial detectors. *Chem Geol*, vol. 45, pp. 145-155. https://doi.org/10.1016/0009-2541(85)90042-7.

18 Ebihara M. (1987) Determination of ten lanthanides in chondritic meteorites by radiochemical neutron activation analysis using coaxial and planar type Ge detectors. *J Radioanal Nucl Chem*, vol. 111, pp. 385-397. https://doi.org/10.1007/BF02072871.

19 Labrecque J.J., Rosales P.A., Mejias G. (1986) Instrumental neutron activation analysis of river sediments from Rio Tigre (Venezuela) employing a planar germanium detector. *Appl Spectrosc*, vol. 40(8), pp. 1232-1235. https://doi.org/10.1366/0003702864507648.

20 Kaizer J., Kučera J., Kameník J., et al. (2017) Determination of elemental content in the Rumanová, Uhrovec, Vel'ké Borové, Košice and Chelyabinsk chondrites by instrumental neutron activation analysis. *J Radioanal Nucl Chem*, vol. 311(3), pp. 2085-2096. https://doi.org/10.1007/s10967-017-5168-3.

21 Mizera J., Řanda Z. (2010) Instrumental neutron and photon activation analyses of selected geochemical reference materials. *J Radioanal Nucl Chem*, vol. 284(1), pp. 157-163. https://doi.org/10.1007/s10967-010-0447-2.

22 Araújo M.F., Corredeira C., Gouveia A. (2007) Distribution of the rare earth elements in sediments of the Northwestern Iberian Continental Shelf. *J Radioanal Nucl Chem*, vol. 271(2), pp. 255-260. https://doi.org/10.1007/s10967-007-0201-6.

23 De Corte F. (2001) The standardization of standardless NAA. *J Radioanal Nucl Chem*, vol. 248(1), pp. 13-20. https://doi.org/10.1023/A:1010601403010.

24 Lin X., Henkelmann R. (2004) The internal comparator method. *Anal Bioanal Chem*, vol. 379, pp. 210-217. https://doi.org/10.1007/s00216-004-2557-6.

25 Silachyov I.Yu. (2020) Combination of neutron activation analysis with X-ray fluorescence spectrometry for the determination of rare-earth elements in geological samples. *J Analyt Chem*, vol. 75(7), pp. 878-889. https://doi.org/10.1134/S106193482007014X.

26 Tiwari S., Nair A.G.C., Acharya R., et al. (2007) Analysis of uranium bearing samples for rare earth and other elements by k_0-based internal monostandard INAA method. *J Nucl Radioch Sci*, vol. 8(1), pp. 25-30. https://doi.org/10.14494/jnrs2000.8.25.

27 Weng Z., Jowitt S.M., Mudd G.M., et al. (2015) A detailed assessment of global rare earth element resources: opportunities and challenges. *Econ Geol*, vol. 110(8), pp. 1925-1952. https://doi.org/10.2113/econgeo.110.8.1925.

28 Koltochnik S.N., Sairanbayev D.S., Chekushina L.V., et al. (2018) Comparison of neutron spectrum in the WWR-K reactor with LEU fuel against HEU one. *NNC RK Bulletin* [Vestnik NYATS RK], vol. 76(4), pp. 14-17 (in Russian).

29 Potts P.J. (1992) A handbook of silicate rock analysis. Springer Science & Business Media, 622 p. ISBN 978-1-4615-3270-5.

30 Greenberg R.R., Bode P., De Nadai Fernandes E.A. (2011) Neutron activation analysis: A primary method of measurement. *Spectrochim Acta Part B*, vol. 66, pp. 193-241. https://doi:10.1016/j.sab.2010.12.011.

31 k_0-News. Nuclear data sub-committee. http://www.kayzero.com/k0naa/k0naaorg/Nuclear_Data_SC/Nuclear_Data_SC.html (10.11.2020).

32 Chilian C., St-Pierre J., Kennedy G. (2008) Complete thermal and epithermal neutron self-shielding corrections for NAA using a spreadsheet. *J Radioanal Nucl Chem*, vol. 278(3), pp. 745-749. https://doi.org/10.1007/s10967-008-1604-8.

33 Shirai N., Hidaka Y., Yamaguchi A., et al. (2015) Neutron activation analysis of iron meteorites. *J Radioanal Nucl Chem*, vol. 303(2), pp. 1375-1380. https://doi.org/10.1007/s10967-014-3654-4.

34 Hubbell J.H., Seltzer S.M. X-ray mass attenuation coefficients. NIST standard reference database 126. https://www.nist.gov/pml/x-ray-mass-attenuation-coefficients (10.11.2020).

35 Diaz O., Figueiredo A., Nogueira C., et al. (2005) Epithermal neutron flux characterization of the IEA-R1 research reactor, Sao Paulo, Brazil. *J Radioanal Nucl Chem*, vol. 266(1), pp. 153-157. https://doi.org/10.1007/s10967-005-0885-4.

36 OST 41-08-212-04 (2004) Standart otrasli. Upravlenie kachestvom analiticheskih rabot. Normy pogreshnosti pri opredelenii himicheskogo sostava mineralnogo syr'ya i klassifikatsiya metodik laboratornogo analiza po tochnosti rezultatov

(Idustrial standard. Quality management of analytical work. Error guidelines for chemical analysis of mineral resources and precision classification of laboratory analytical techniques). Moscow, VIMS, 23 p. (in Russian).

37 ISO 13528:2015 (2015) Statistical Methods for Use in Proficiency Testing by Interlaboratory Comparisons. Genève, Switzerland, 89 p.

38 Omirserikov M.Sh., Yusupova U.Y., Togizov K.S., et al. (2015) Rare earth elements in the weathering crust of Shock-Karagai deposit (North Kazakhstan). *News of the Academy of Sciences of RK*, *ser*. *geol*., vol. 3, pp. 35-41. (in Russian).

39 Omirserikov M., Stepanenko N., Pankratova N., et al. (2015) Redkometalnye i redkozemelnye mestorozhdenia Kazahstana (Rare metal and rare earth deposits of Kazakhstan). http://metalmininginfo.kz/archives/2256 (25.08.2020). (in Russian).